Ethylenediannine Grafting on Oxide-Free H-, 1/3 ML F-, and Cl-Terminated Si(111) Surfaces

ARTICLE *in* CHEMISTRY OF MATERIALS · SEPTEMBER 2015

Impact Factor: 8.35 · DOI: 10.1021/acs.chemmater.5b03156

6 AUTHORS, INCLUDING:

Tatiana Peixoto Chopra
University of Texas at Dallas
11 PUBLICATIONS **47** CITATIONS
SEE PROFILE

Kyeongjae Cho
University of Texas at Dallas
302 PUBLICATIONS **9,389** CITATIONS
SEE PROFILE

Mathew D. Halls
Schrödinger Inc.
63 PUBLICATIONS **2,390** CITATIONS
SEE PROFILE

Peter Thissen
Karlsruhe Institute of Technology
33 PUBLICATIONS **489** CITATIONS
SEE PROFILE

CHEMISTRY OF MATERIALS

Article

pubs.acs.org/cm

Ethylenediamine Grafting on Oxide-Free H-, 1/3 ML F-, and Cl-Terminated Si(111) Surfaces

Tatiana Peixoto Chopra,[†] Roberto Carlos Longo,[†] Kyeongjae Cho,[†] Mathew D. Halls,[‡] Peter Thissen,[§] and Yves J. Chabal*[,†]

[†]Department of Materials Science and Engineering, University of Texas at Dallas, Richardson, Texas 75080, United States

[‡]Materials Science Group, Schrödinger Inc., San Diego, California 92121, United States

[§]Institute of Functional Interfaces, Karlsruhe Institute of Technology, Karlsruhe, Germany

Supporting Information

ABSTRACT: Amine termination of surfaces constitutes a core platform for fields as diverse as microelectronics and bioengineering, and for nanotechnology in general. Diamines are particularly attractive for surface amination because unlike ammonia or simple amine molecules, they have a metal chelating capability useful in fabricating heterostructures. They can act as a linker molecule between inorganic electronic materials and biomolecules or photoactive quantum dots for applications in microelectronic, photonics, and biosensing. In contrast to ammonia modification of silicon surfaces, the direct grafting of diamine on silicon surfaces has been less explored. In this work, the attachment of liquid and vapor-phase ethylenediamine (EDA) on three types of oxide-free (H-, 1/3 ML F-, and Cl-terminated) Si(111) surfaces is therefore examined by infrared absorption spectroscopy and X-ray photoelectron spectroscopy in conjunction with first-principle calculations. We find that EDA chemisorption is only possible on 1/3 ML F- and Cl-terminated Si(111) surfaces: EDA only physisorbs on H-terminated Si(111) surfaces. On Cl-terminated Si(111) surfaces, EDA molecules adsorb in a mixture of monodentate and bridging configurations (chemical reaction of both EDA end groups), while on 1/3 ML F-terminated Si(111) surfaces the adsorption occurs primarily at one end of the molecule. EDA reaction with Cl-terminated Si(111) surfaces is also characterized by complete removal of Cl and partial Si−H (~25% ML) formation on the surface. This unexpected Si−H product suggests that a proton−chlorine exchange may take place, with the endothermic barrier possibly reduced via concerted chemical reactions after an initial attachment of EDA to the surface.

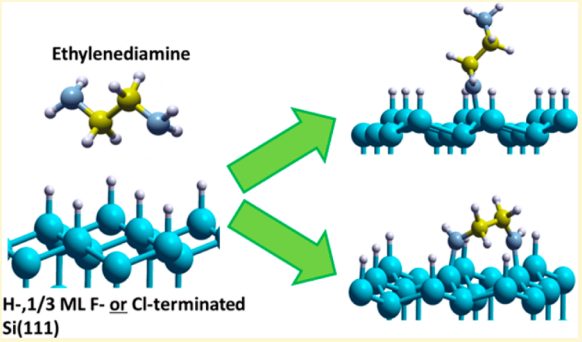

1. INTRODUCTION

Amination of surfaces have been critical for a variety of applications including microelectronics (surface functionalization),[1−4] biotechnology (biomolecules attachment),[5−8] and nanotechnology (nanoparticles attachment).[1,6,9,10] Ammonia has initially been most commonly used for silicon nitridation and amination, with most of the literature focused on the vapor phase dissociation of ammonia on clean reconstructed Si(100) 2×1[11−17] or Si(111) 7×7 surfaces.[14,18−20] Another standard way for amination is derived from the ammonia or amine decomposition on modified silicon, such as the stepwise NH_3 vapor dissociation on H-terminated Si(111) surfaces[21] or the ammonia/amine reactions on Cl-terminated Si(100) or Si(111) surfaces in vapor[22−24] and liquid[24−27] phases. Later, organic amines have attracted interest in the fields of biochemistry and nanotechnology for their ability to functionalize surfaces. For instance, amines such as aminosilanes[1,5,6,8] and diamines[7,9,10] can act as linkers to attach nanoparticles, quantum dots, or biomolecules, enabling the development of advanced biosensors and solar cells.[1−3,6,9,10]

Among organic amines, diamines are particularly interesting, in part because they enable reactions only possible with this bifunctionality. For instance, in some applications it is useful to have one of the two NH_2 end groups reacts with the substrate, with the second end group remaining open for further reactions. Specifically, ethylenediamine (EDA) has proven to be useful for a variety of applications, as (i) a chelating agent for metals by reaction of both NH_2 end groups with the metal center,[28,29] acting as a complexing agent or a linker to a sensor gate; (ii) a capping agent for porous metal complexes allowing them to absorb molecules in solution, thus creating a regularly ordered crystal structure through the molecular absorption process;[30] (iii) a coordination ligand to produce highly uniform CuS structures with high photocatalytic performance;[2] (iv) a molecular binder between $[Fe_{16}S_{20}]^{4-}$layers, creating a brand new family of semiconductor materials with significantly

Received: May 21, 2015
Revised: September 3, 2015

DOI: 10.1021/acs.chemmater.5b03156
Chem. Mater. XXXX, XXX, XXX−XXX

enhanced properties, including reduced thermal conductivity and a low optical bandgap (~0.7 eV);[3] (v) a modulator of the electric field on grafted nanocrystals in CdSe-based solar cells, enhancing the performance of the solar cell;[9] (vi) an agent to foster the synthesis of a self-assembled, closely packed, columnar-arranged DNA complex that is noninterferon inducing;[7] (vii) ligands in metal−organic frameworks (MOFs) for the capture of CO_2 gas, showing a high gas capture capacity;[31−33] and (viii) a key molecule to prepare polyethylenimine (PEI) polymer created by anodic oxidation (>4 eV energy necessary) that can be used be used as a conductive coating for biosensors.[34−38] In all of these applications, further characterization of EDA attachment configuration would provide essential insight toward enhancing the properties displayed by the EDA-modified product. Yet, in contrast to its parent molecule, NH_3, relatively little work has been done on the direct attachment of diamines to silicon surfaces, despite the ability of its symmetrical bifunctionality to foster a more organized and controlled fabrication of nanostructures on the semiconductor surface.

To systematically study EDA attachment at surfaces, chemically and structurally well-defined surfaces are required. This is possible for silicon (Si) surfaces, in particular atomically flat Si(111) surfaces that can be prepared with three distinct terminations (H-, 1/3 ML F-, and Cl-termination), and therefore represent a good starting point for these surface studies. The atomically flat Si(111)-H surface has been used and studied for decades[39−41] and shown to be an ideal substrate to graft alkene-terminated molecules by hydrosilylation.[5,6] Fluorination of Si is more difficult as fluorine tends to etch silicon very easily. However, starting from an atomically flat H-terminated Si(111) surface, Michalak et al.[42] have developed a method to produce a mixed surface with 1/3 ML F- and 2/3 ML H-termination (where ML stands for monolayer), remaining atomically flat and stable through numbers of wet chemical steps. Because the Si−F bond is surrounded by a ring of six Si−H bonds, this is an excellent model surface to compare the relative reactivity of amines with Si−F and Si−H surface groups. On the premise that Si−F reacts faster than Si−H with amines,[23] this model surface is also ideal to study reactions with isolated Si−F groups. Finally, complete chlorination of H-terminated Si(111) surfaces has been demonstrated, either using wet chemistry or with gas phase chlorine, without roughening the surface.[24,43,44]

In this work, we use both liquid and gas phase processing to attach EDA on these three well-defined H- and 1/3 ML F- and Cl-terminated Si(111) surfaces. We find that, while no chemisorption is possible on H-terminated Si(111) surfaces, EDA can react with both 1/3 ML F- and Cl-terminated Si(111) surfaces albeit differently. It attaches in a monodentate fashion (only one amine end reacted) on 1/3 ML F-terminated Si(111) surfaces with free NH_2 groups on the opposite end; on Cl-terminated Si(111) surfaces, the adsorption involves a mixture of mono and bidentate configurations, as evidenced by distinct IR signatures and a reduction of free NH_2 end groups. Unexpectedly, we also observe the formation of Si−H bonds on Cl-terminated Si(111) surfaces after diamine exposure and complete removal of all Cl. First-principles modeling of this complex system suggests that there may be a proton−chlorine exchange under certain circumstances, despite the endothermic nature of this reaction.

2. METHODS

Experimental Details. Anhydrous methanol (CH_3OH, 99.8%), anhydrous redistilled ethylenediamine (EDA, $NH_2(CH)_2NH_2$, ≥ 99.5%), phosphorus pentachloride (purum p.a., PCl_5, ≥ 98.0%), and anhydrous toluene ($C_6H_5CH_3$, 99.8%) were purchased from Sigma-Aldrich. These chemicals were placed inside a $N_2(g)$-purged glovebox prior to use. Aqueous ammonium fluoride (40 wt %) and aqueous hydrofluoric acid (49 wt %) were obtained from J.T. Baker. Aqueous hydrogen peroxide (30 wt %) and concentrated (18 M) sulfuric acid were obtained from Fisher Scientific. All deionized H_2O was obtained from a Millipore Advantage A10 water filtration system, characterized by a resistivity of 18.2 MΩ·cm. N-type (phosphorus-doped, resistivity of 24−34 Ω·cm) float-zone double-side polished Si(111) wafers were cut into 1.5 cm × 3.8 cm pieces for infrared transmission and XPS measurements.

The initially oxidized silicon samples were chemically cleaned by a 30 min immersion in an 80 °C solution of 3:1 concentrated (18 M) H_2SO_4/30% H_2O_2(aq) (hereafter referred to as a piranha solution) to remove organic contamination. Si(111) samples were hydrogen terminated by a 30 s dip in 10−20% HF(aq) followed by a 2.5 min dip in 40% NH_4F(aq), and a final rinse in H_2O for 10 s.[45] This latter procedure produces an atomically smooth surface for tens to hundreds of nanometers depending on the sample miscut. Si(111) samples were often reused since atomically flat surfaces can be reformed by intermediate reoxidation. A partially fluorinated (1/3 ML F-) termination on H-terminated Si(111) samples, henceforth referred to as the 1/3 ML F-terminated Si(111) surface, was achieved using the method of Michalak et al.[42] based on intermediate methoxylation in methanol and HF etching. The Cl-terminated Si(111) surfaces were prepared using a wet chemical methods previously described in the literature.[43,46] Once the oxide-free Si(111) surfaces were passivated by H, 1/3 ML F and 2/3 ML H, or Cl, further functionalization was performed inside a nitrogen glovebox either using 14 mL of neat ethylenediamine in a glass vial for 30 min at room temperature in the dark or a 20 mM ethylenediamine/toluene solution. Alternatively, vapor phase experiments were conducted in a stainless steel chamber with a base pressure of ~10^{-6} Torr, at an ethylenediamine pressure of 1.2 Torr for 3 min, followed by $N_2(g)$ purge for 180 s. *In-situ* infrared measurements were performed in this chamber, equipped with KBr windows, with spectral measurements taken at 80 °C for all vapor phase experiments.

IR absorption data were recorded in the dry $N_2(g)$-purged bench of a Fourier transform infrared (FTIR) spectrometer (Nicolet 6700). Spectra were obtained with a nominal 4 cm^{-1} resolution between 400 and 4000 cm^{-1} in transmission, at an angle of incidence of 74° with respect to the Si(111) surface normal. A room temperature pyroelectric detector (DTGS) was used for data collection. Three consecutive loops, each consisting of 500 single beam spectral scans, were obtained for each sample. Reference spectra were obtained on the respective starting surfaces, such as H-,1/3 ML F-, or Cl-terminated Si(111) and on the original oxidized surfaces. Differential spectra are defined as the spectra of the previous functionalization step used as a reference.

XPS analysis was performed *ex-situ* with a Quantum 2000 Scanning ESCA Microprobe (Physical Electronics, USA) spectrometer equipped with a concentric hemispherical analyzer under ultrahigh vacuum conditions (10^{-9} mbar) and an Al Kα X-ray source (15 keV, filament current 20 mA). Spectra were recorded at a 45° takeoff angle with respect to the surface. A sample area of 100 μm × 100 μm was analyzed using a pass energy of 29.25 eV for the detailed elemental scans. The spectra obtained were analyzed using the CASA XPS software. The monolayer coverage was calculated using the method outlined by Michalak et al.,[42] and the silicon oxide layer thickness was calculated using the overlayer-substrate method outlined in Himpsel et al.,[47] with a detailed description for each calculation found in the Supporting Information.

For each of the surface terminations, the error bars associated with the estimated coverages were calculated by taking the standard deviation of the calculated coverage in three independent samples.

DOI: 10.1021/acs.chemmater.5b03156
Chem. Mater. XXXX, XXX, XXX−XXX

Liquid-phase EDA reacted samples in a nitrogen-purged atmosphere or vapor-phase EDA reacted samples in a vacuum (10^{-6} Torr chamber) were either measured immediately with IR spectroscopy (no atmospheric exposure) or taken to the XPS chamber (i.e., exposed to the atmosphere for ~1 min before vacuum introduction). In cases where surface charging was suspected, XPS charge correction was done by setting the C 1s peak to 285 eV and correcting all other core level peaks accordingly.

Computational Details. First-principles calculations were performed using density-functional theory (DFT) as implemented in the Vienna *Ab initio* Simulation Package (VASP)[48,49] code within the Projector-Augmented Wave (PAW) approach.[50] The total energy calculations were performed using the Perdew–Burke–Ernzerhof (PBE) generalized-gradient approximation (GGA) functional,[51] and the electronic wave functions were expanded into plane waves up to a kinetic energy of 400 eV. The supercell used in this work consists of 8 atomic layers of H- or Cl-terminated Si(111) surface plus adsorbed molecules and a vacuum region equivalent to 16 atomic layers. The 7 uppermost layers of Si as well as the adsorbate degrees of freedom were allowed to relax without any constraint to a tolerance of 10^{-4} eV in the total energy and 0.01 eV/Å in the forces on every atom. For all of the structures considered, a Brillouin zone sampling with a 4 × 4 × 1 *k*-point mesh within the Monkhorst–Pack scheme[52] was used to ensure a convergence of 1 meV/unit cell.

The Eigenmodes and the vibrational frequencies were obtained with the force-constant (FC) approach, diagonalizing the mass-weighted second derivative matrix (Hessian) in case of the adsorbed species and the top Si layer. The restriction to the atoms of the top layer and the adsorbed species is legitimate because the Eigenmodes of these atoms do not overlap with the Eigenmodes of the bulk material. The kinetic barriers, transition states, and reaction pathways were obtained using the climbing image-nudged elastic band method (CI-NEB).[53−55] This method has previously been shown to be reliable in obtaining the minimum energy path (MEP) between a set of two different states, where the reaction path is divided into a set of images "connected with a spring." During the relaxation, the initial and final states are kept frozen while the images move according to the constraint of the "elastic band." The MEP is then found when the components of the forces perpendicular to the "elastic band" vanish, the relative positions of the images and the barrier being determined by the parallel components of the forces.[53,54]

3. RESULTS

A. Ethylenediamine Interactions with H-,1/3 ML F-, and Cl-Terminated Si(111) Surfaces. Infrared absorption spectroscopy is most useful in determining the bonding configuration of adsorbed molecules through the detection of their molecular vibrations and the molecule–surface bonds in the cases of chemisorption. The summary of IR absorption spectra obtained upon ethylenediamine (EDA) processing of these three model surfaces is shown in Figure 1 and discussed sequentially below.

i. Adsorption on the H-Terminated Si(111) Surface. When EDA is exposed to a H-terminated Si(111) surface (Figure 1B), almost no characteristic amine vibrations are observed except for a weak NH_2 scissor deformation band at 1595 cm^{-1} and a weak ν(Si–N) stretch vibration at 825 cm^{-1}. Instead, there is a relatively stronger absorption band in the 1000–1200 cm^{-1} region attributed to ν(Si–O) stretch modes, possibly due to oxidation of the substrate during the reaction. This oxide band hinders the detection of ν(C–N) stretch vibrations (1020–1100 cm^{-1}) that are known to be weak[56,57] and therefore cannot be easily distinguished.

ii. Adsorption on the 1/3 ML F- and 2/3 ML H-Terminated Si(111) Surface. The situation is different for 1/3 ML F-terminated Si(111) surface.[42] When exposed to liquid EDA under similar conditions, the differential infrared spectra of the resultant surface (Figure 1A) shows several amine related modes. The two modes from the symmetric and antisymmetric NH_2 stretch modes at 3230 and 3350 cm^{-1} are discernible, and the scissor NH_2 deformation mode at 1595 cm^{-1} is clearly visible.[58] A weak yet detectable ν(Si–N) stretch vibration is present at 825 cm^{-1} along with the ν(C–H) symmetric and antisymmetric stretch vibrations at 2888 and 2934 cm^{-1}, respectively, further confirming the attachment of the molecule on the surface.

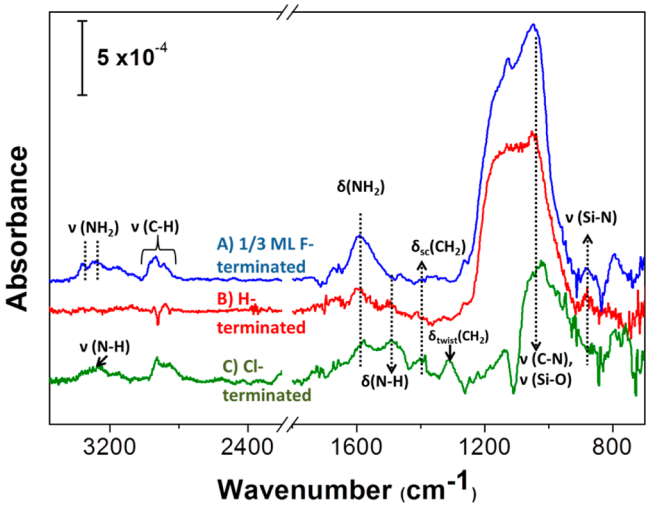

Figure 1. Differential transmission infrared spectra showing ethylenediamine attachment on (a) 1/3 ML F-, 2/3 ML H-terminated Si(111), (b) H-terminated Si(111), and (c) Cl-terminated Si(111) surface. All spectra are referenced to their respective surface termination.

iii. Adsorption on the Cl-Terminated Si(111) Surface. For the Cl-terminated Si(111) surface, the spectrum contains features not found in the other two surfaces (Figure 1C). Some absorption bands are similar to the other terminations, such as the scissor NH_2 deformation mode at 1595 cm^{-1}, a band at 3290 cm^{-1} associated with the ν(N–H) stretch vibration of secondary amines (i.e., only one hydrogen on the nitrogen atom), and also the ν(C–H) symmetric and antisymmetric modes at 2868 and 2930 cm^{-1}. There are also five new vibrations found: three at 1493, 1423, and 1316 cm^{-1} attributed to the δ_{wag}(N–H) deformation mode,[57,58] δ(C–H_2) deformation mode, and δ_{twist}(C–H_2) deformation mode,[56,58] respectively, and two more at 2050 cm^{-1} (shoulder) and 623 cm^{-1} attributed to the stretch and deformation vibrational modes of a newly formed Si–H (shown in Figures 8 and S1) on the original Cl-terminated and H-free Si(111) surface (see Figure 8). As discussed later, the first three bands point to a specific bonding configuration involving the reaction of both ends of the diamine molecule, while the Si–H bond formation involves an alternate chlorine–EDA reaction pathway that may dominate after the initial diamine reaction takes place. To address the interaction with the Cl-terminated Si(111) surfaces first, the next section starts in the reverse order.

B. XPS of Ethylenediamine on H-, 1/3 ML F-, and Cl-Terminated Si(111) Surfaces. To better understand the IR absorption results, X-ray photoelectron spectra were acquired for each different surface termination and presented below in a reverse order. All estimates of the coverage were performed using the calculation method described by Michalak et al.[42] and

DOI: 10.1021/acs.chemmater.5b03156
Chem. Mater. XXXX, XXX, XXX–XXX

the oxide layer thickness using the method of Himpsel et al.[47] both outlined in the Supporting Information.

i. Adsorption on the Cl-Terminated Si(111) Surface. As seen in Figure 2A, upon adsorption of EDA on chlorinated

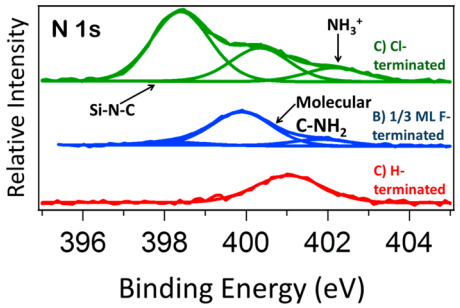

Figure 2. XPS of ethylenediamine on different surface terminations showing evidence of monodentate and/or bridge attachment for the Cl-terminated Si(111) surface with some charging/dative bonding occurring (A), the 1/3 ML F-terminated Si(111) surface containing a mixture of multilayers and signal from the tail (NH_2) belonging to monodentate attachment, obscuring the Si−N−C signal from below (B), and only charged/dative bonded species (NH_3^+, Si-NH_2^+-C) observed on the H-terminated Si(111) surface (C).

surfaces, three characteristic peaks are observed in the N 1s region at (1) 398.5 eV attributed to a Si−N−C attachment, (2) 400.4 eV a monodentate C-NH_2 attachment (or merely physisorbed molecular species), and (3) 402.1 eV to dative bonding or a charged molecule, possibly through interaction with the leaving chlorine atom.[14,18−20,59] We estimate the nitrogen coverage to be 0.9 ± 0.2 ML based on the area of the N 1s peak, and 0.84 ± 0.04 ML based on the signal fitted for the Si^{1+} 2p peak (not shown, found at 100.0 eV, accounts for contributions from Si−N, Si−O, or Si−Cl), thus showing a similar amount of coverage in both calculations. The Si−Cl surface contains a 0.22 ± 0.4 nm oxide layer thickness which is ∼10× less when compared to a native oxide surface (2.1 nm). The oxide layer peak present in the Si 2p XPS spectra (Figure 3C) was found at 102.9 eV being +3.7 eV higher than the Si

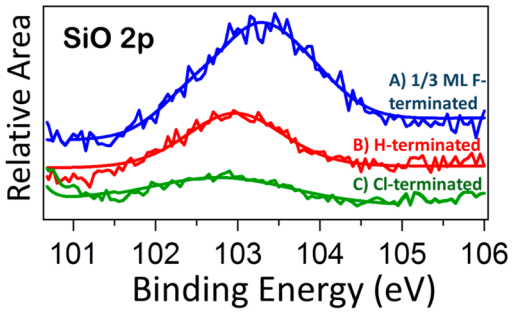

Silicon Oxide on Surface	Thickness (nm)	% Concentration
H-terminated Si(111)	1.4 ± 0.6	27 ± 9
1/3 ML F-terminated Si(111)	0.9 ± 0.3	18 ± 5
Cl-terminated Si(111)	0.2 ± 0.1	5 ± 1

Figure 3. XPS spectra of the Si 2p region of ethylenediamine on (a) 1/3 ML F-terminated Si(111) surface, (b) H-terminated Si(111) surface, and (c) Cl-terminated Si(111) surface, including calculated oxide thickness and % concentration from the Si 2p region. Each spectrum was normalized to its Si bulk peak height for comparison of the oxidation levels for each surface termination.

$2p^{2/3}$ bulk peak binding energy, fixed at 99.2 eV for all terminations. This distance from the bulk peak is indicative of a Si^{4+} oxidation state and is in good agreement with the value of +3.9 eV for this oxidation state reported by Himpsel et al.[47]

It is assumed that this backbonded oxidation occurred due to trace amounts of oxygen-containing groups either during immersion in the neat EDA liquid or upon exposure to air for *ex-situ* XPS analysis.

ii. Adsorption on the 1/3 ML F-Terminated Si(111) Surface. For the 1/3 ML F-terminated Si(111) surfaces, there are only two distinguishable N 1s peaks (Figure 2B): a main contribution at 399.8 eV attributed to C-NH_2 and a weaker contribution at 401.6 eV indicative of dative bonding or charging of the NH_2 end groups. The surface coverage is estimated at 0.7 ± 0.2 ML based on the integrated area of the N 1s core level. However, a N coverage of only 0.28 ± 0.06 ML is calculated using the Si^{1+} 2p peak at 99.9 eV (not shown). The estimated coverage calculated using the Si 2p is closer to the expected 1/3 ML F surface termination, although the signal could be from a Si−N, Si−O, and/or a remnant Si−F termination. Because of the relatively high coverage calculated by the N 1s core level and with the 1/3 ML Si^{1+} coverage remaining relatively the same, if the fluorine was replaced this suggests that a monodentate reaction may have taken place. Unlike the Si−Cl surface, the 1/3 ML Si−F surface has a level of oxidation estimated at 0.9 ± 0.3 nm thick, with a clear oxide peak seen in Figure 3A found at 103.2 eV (in good agreement with the binding energy of 103.3 eV seen for native silicon oxide).

iii. Adsorption on the H-Terminated Si(111) Surface. On the H-terminated Si(111) surface, only datively bonded/charged EDA species are observed. Figure 2C shows only one binding energy for the N 1s core level, located at 401.0 eV with an estimated EDA coverage of 0.9 ± 0.5 ML. If we use the Si^{1+} peak found at 99.8 eV (not shown) instead, the estimated coverage is 0.08 ± 0.08 ML, supporting the N 1s core level assignment and indicating a lack of reaction. The silicon oxide peak at 103 eV is consistent with surface oxidation (see Figure 3B), with an estimated 1.4 ± 0.6 nm thick layer (the surface is likely very inhomogeneous). Since the EDA appears to be physisorbed and the surface oxidized, the next section explores the dependence on EDA concentration with the hope of reducing surface oxidation.

C. Dependence on Ethylenediamine Concentration for EDA Adsorption on H-Terminated Si(111) Surfaces.

In an effort to reduce the amount of charged EDA on the surface and the overall surface oxidation, a lower solution concentration (20 mM) was used. Instead of using neat EDA, a 20 mM solution was prepared in toluene with a 30 min exposure at room temperature. Figure 4 shows that the characteristic EDA vibrations are still observed: NH_2 stretch modes at 3160 and 3265 cm^{-1} and NH_2 deformation mode at 1590 cm^{-1}, together with modes at 2880, 2940, and 1455 cm^{-1} associated with the symmetric and antisymmetric stretches and deformation modes of CH_2, respectively. The IR spectrum in the inset of Figure 4 shows that 86% ± 5% ML hydrogen remains on the surface with an Si−H stretch frequency at 2083 cm^{-1} as in the original surface. There is only minor oxidation evidenced by the ν (O_xSi−H) stretch mode at 2270 cm^{-1} and the weak but observable XPS Si 2p peak at 102.5 eV, estimated at 0.15 ± 0.01 nm average thickness. The absence of a Si^{1+} peak at 0.7−0.9 eV away from the Si bulk peak suggests that there is no detectable amine attachment to the surface. This is

DOI: 10.1021/acs.chemmater.5b03156
Chem. Mater. XXXX, XXX, XXX−XXX

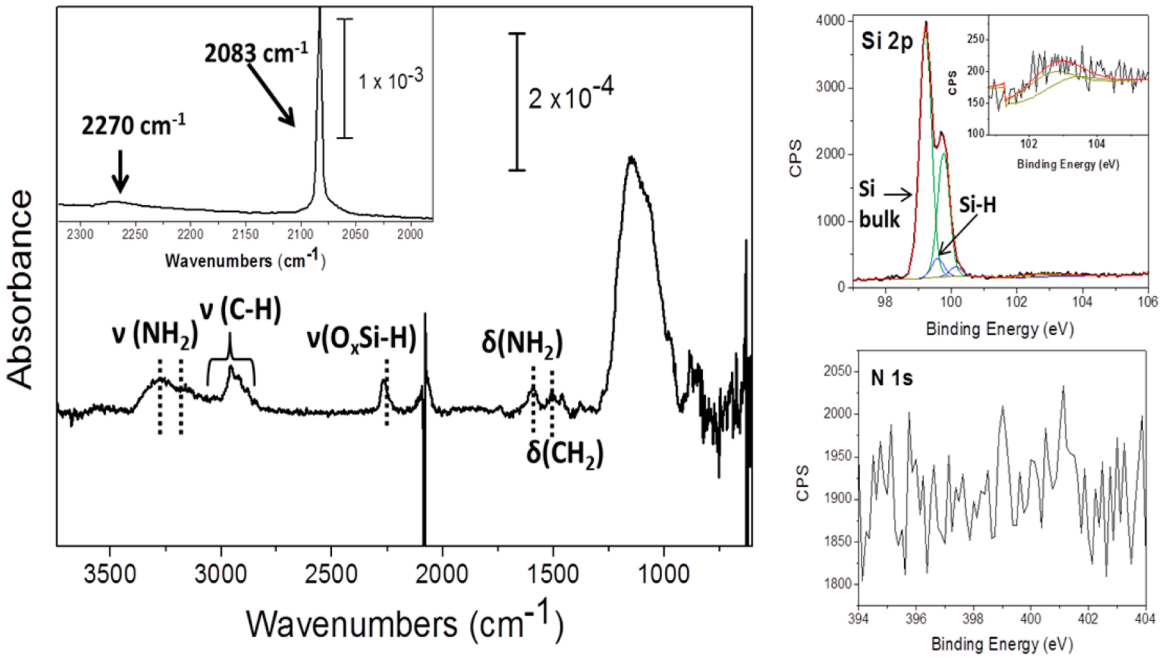

Figure 4. XPS of Si 2p and N 1s core levels and IR spectra of 20 mM ethylenediamine solution in toluene reacted at room temperature with a H-terminated Si(111) surface, showing signature vibrations of the diamine with minimal silicon oxidation and negligible signs of nitrogen via XPS.

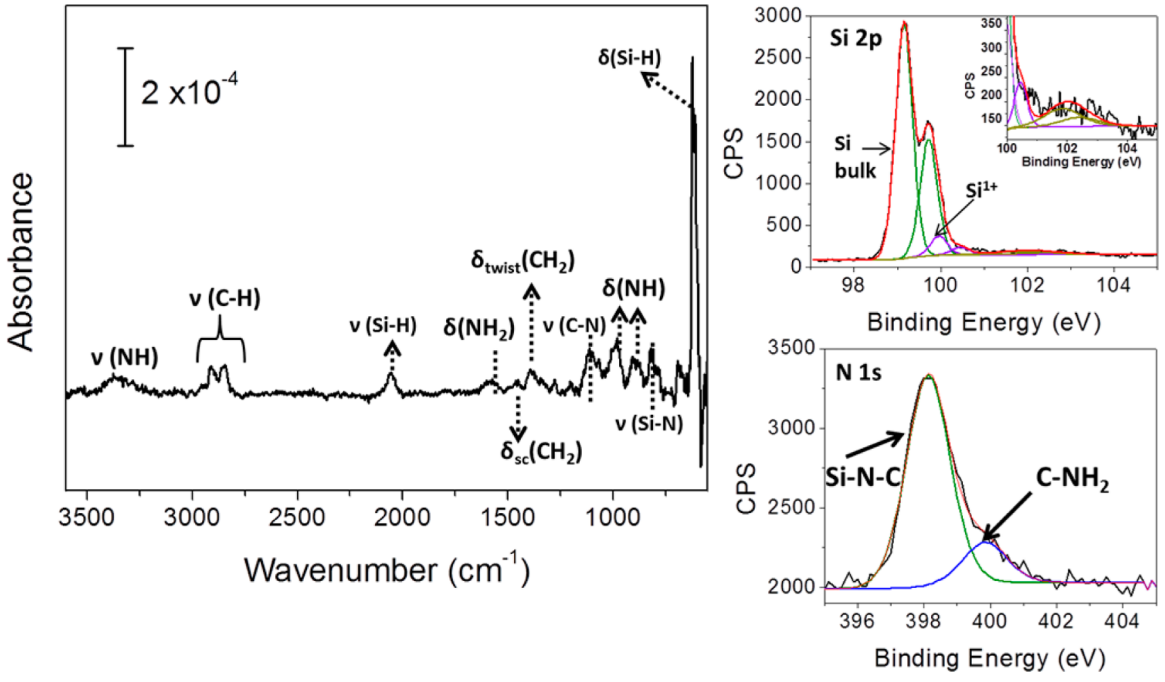

Figure 5. Vapor phase infrared spectroscopy and XPS of ethylenediamine (EDA) reacting with a full Si(111)-Cl surface at a sample temperature of 350 °C. Referenced to the starting Cl-terminated Si(111) surface.

confirmed by the absence of nitrogen in the XPS N 1s spectra and suggests that the observed EDA infrared signal originated from physisorbed molecules which desorbed under vacuum conditions.

D. Vapor-Phase EDA on 1/3 ML F- and Cl-Terminated Si(111) Surfaces. Examining the adsorption of vapor-phase EDA on 1/3 ML F- and Cl-terminated Si(111) surfaces provides useful complementary information to better understand their surface reactivity. Instead of varying the concentration as done in the wet chemical treatments, the parameter varied in the vapor phase treatment is surface temperature, with the limit being the H-, F-, or Cl-desorption temperatures. For H-termination, as in the case of NH_3, reaction can only occur very close to desorption and leads to ambiguous results. We focused on the 1/3 ML F- and Cl-terminated Si(111) surfaces since F and Cl desorption temperatures are higher and reaction barriers lower than for H-terminated Si(111) surfaces, with their reaction results summarized in Figures 5 and 6.

DOI: 10.1021/acs.chemmater.5b03156
Chem. Mater. XXXX, XXX, XXX−XXX

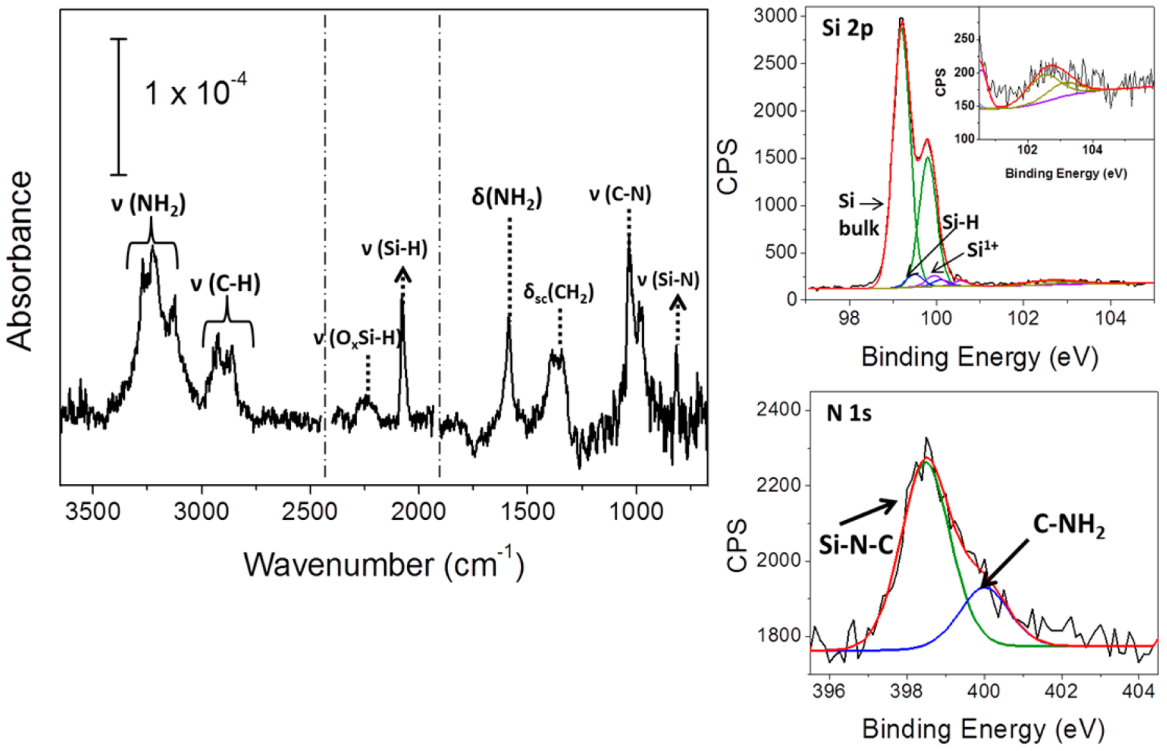

Figure 6. Vapor phase infrared spectroscopy and XPS spectra of ethylenediamine (EDA) reacting with the 1/3 ML F-terminated Si(111) surface at a sample temperature of 350 °C. Referenced to the 1/3 ML F-terminated Si(111) surface after a surface preanneal to 350 °C before EDA exposure of the regions of 2500−3550 cm^{-1} and 700−1850 cm^{-1} and to the oxide surface for the 1900−2400 cm^{-1} region.

Cl-Terminated Si(111) Surface. The IR absorption spectrum shows a clear and sharp band at 824 cm^{-1} corresponding to the ν(Si−N) vibration. This provides clear evidence for the reaction of amine groups to the Si−Cl surface. In addition, the spectrum is characterized by a broad ν(N−H) band at 3340 cm^{-1}, two ν(C−H) bands at 2918 and 2850 cm^{-1}, and δ(NH) bands at 980 and 895 cm^{-1}. The vapor phase experiment also shows distinct peaks associated with ν(C−N) at 1112 cm^{-1} characteristic of secondary amines and modes associated with the alkane chain at 1395 cm^{-1} for the $\delta_{twist}(CH_2)$ and 1460 cm^{-1} for the $\delta_{sc}(CH_2)$, as also observed for the wet treated surfaces (see Figure 1 C). There are also bands corresponding to NH_2, such as the $\delta(NH_2)$ band at 1580 cm^{-1}. Surprisingly, just as observed with wet chemical treatments, there are clear bands at 2060 and 623 cm^{-1} corresponding to the Si−H stretch and bend bands, respectively, formed upon vapor EDA exposure. Comparison of their integrated areas with those of a H-terminated Si(111) surface yields a surface coverage of 19% ± 1% ML.

The N 1s core level spectrum in Figure 5 (right panel) is consistent with the predominance of Si−N−C bonds, and a small concentration of C-NH_2 species, having a NH-C/H_2N−C peak ratio of 17:3. Assuming this surface does not contain physisorbed EDA molecules (Figures 5 and 6 show similar ν(C−N) infrared intensities and no XPS N 1s charged species), this ratio indicates that for every 20 nitrogen signals detected, a monodentate attachment contributes 3 parts from its C-NH_2 end group, and 3 parts contributed to the H−N−C/Si−N−C peak via the Si-NH-C bond formed. The remaining 14 parts (i.e., 17−3 = 14) of the N 1s NH-C peak can be attributed to a doubly reacted EDA molecule (Si-NH−CH_2−CH_2−NH-Si bridge configuration or monodentate NH_2 end group oxidized to NH upon air exposure). Because there is no evidence of chlorine in the Cl 2p spectra after the EDA exposure (see Figure 7 and Table 1), the Si^{1+} peak is solely due to the Si-NH-

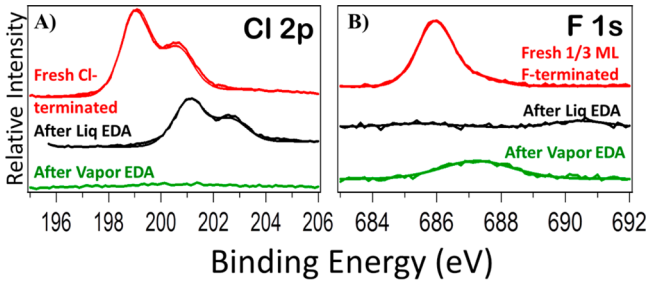

Figure 7. XPS spectra of (a) chlorine and (b) fluorine amount left on the silicon surface after the reaction with ethylenediamine.

Table 1. Ratios of Quantities Left on Substrate before and after Ethylenediamine Reaction at Room Temperature in 30 min for Liquid Phase and 350 °C for Vapor Phase

sample	ratio F/Si	ratio Cl/Si
fresh 1/3 ML F-terminated	0.026 ± 0.001	
1/3 ML F-terminated after liq EDA	0.002 ± 0.001	
1/3 ML F-terminated after vapor EDA at 350 °C	0.012 ± 0.002	
fresh Cl-terminated		0.091 ± 0.001
Cl-terminated after liq EDA		0.053 ± 0.002
Cl-terminated after vapor EDA at 350 °C		0

DOI: 10.1021/acs.chemmater.5b03156
Chem. Mater. XXXX, XXX, XXX−XXX

C moiety; this is also supported in the comparison of monolayer coverage, with the Si^{1+} peak having an estimated 0.9 ± 0.1 ML EDA coverage against a 0.83 ± 0.05 ML of EDA coverage according to the N 1s core level. For the vapor phase experiments, the XPS N 1s peak shows only two peaks at 398.2 and 399.8 eV associated with Si−N−C and C-NH_2 respectively without the charged amine peak found at ∼402 eV for the liquid phase EDA.

Finally, there is a small amount of oxide, as determined from the Si 2p core level spectrum (Figure 5, right panel), which is most likely formed during transport from the vacuum chamber to the XPS chamber (requiring air exposure for at least 1 min; 30 min total time from the vacuum chamber to the beginning of XPS analysis). The estimated oxide layer thickness of 0.14 ± 0.06 nm is believed to be distributed unevenly over the surface and thus leaving most of the surface oxide-free.

1/3 ML F-Terminated Si(111) Surface. The main difference with the 1/3 ML F-terminated Si(111) surfaces are stronger $N-H_2$ vibrations in the IR absorption spectrum (Figure 6), $\nu(N-H_2)$ at 3226 and 3126 cm^{-1}, and a sharp and strong $\delta(NH_2)$ at 1587 cm^{-1}, consistent with a majority of primary amines (free NH_2 end groups) on the surface. Characteristic alkane chain modes at 2924 and 2860 cm^{-1} for the stretch $\nu(C-H_2)$ modes and at 1420 cm^{-1} for the $\delta_{sc}(CH_2)$ mode are also present, although the spectra do not contain some of the bending vibrations seen in the Cl-termination. The presence of a band at 820 cm^{-1} corresponding to ν(Si−N) and a band at 1035 cm^{-1} to ν(C−N) of primary amines indicates that the other end of the EDA has chemically reacted with the surface; most likely the Si−F bond since EDA has been shown not to readily react with the H-terminated Si(111) surface. In fact, the Si−H bands are clearly observed. Moreover, the position of the Si−H stretch is significant. On the starting surface, this mode is at 2092 cm^{-1} due to the close proximity of Si−F moieties.[42] After EDA exposure, the Si−H is characterized by a stretch mode at 2079 cm^{-1}(Figure 6), indicating the F is removed from the surface and replaced by an N or O bond.[42] The IR spectrum reveals that there is also a small amount of oxidation in the backbond of Si−H, as evidenced by the presence of a weak band at 2247 cm^{-1}, corresponding to the $\nu(O_x-Si-H)$ vibration.

The right panels of Figure 6 (XPS data) confirm the formation of Si−N−C bonds (N 1s at 398.5 eV) and C-NH_2 presence (N 1s at 400 eV). In this case, the ratio between the Si−N−C and NH_2 components is a 7:3 ratio. As in the previous section, it is assumed that this surface does not have physisorbed EDA molecules present. Therefore, in this case, a monodentate attachment will show 3 parts of the signal belonging to the NH_2 moiety, with 3 of the 7 parts belonging to the Si-NH-C bond of the monodentate connection. The remaining 4 of the 7 parts can be due to bridge formation on the surface (Si-NH−CH_2−CH_2−NH-Si) or a conversion of the dangling NH_2 moiety to NH upon air exposure (as thoroughly discussed in the Discussion section A (ii). The elemental peaks of the Si 2p are found at 99.2 eV, 99.5 eV, 99.96 eV, and 102.5 eV, corresponding to the Si bulk, Si−H, Si−F, or Si−N for Si^{1+} and silicon oxide, respectively. The estimated EDA coverage of 0.36 ± 0.09 ML by Si^{1+} is comparable to the sum of the signals that contribute to the Si^{1+} peak: 0.25 ± 0.04 ML coverage using only the Si−N−C and the calculated remaining monolayer of fluorine at 0.06 ± 0.02 ML (coverage calculated using all N 1s signal is 0.33 ± 0.03 ML). This surface had a small amount of oxidation, amounting to an estimated 0.12 ± 0.05 nm thickness which might account for the similarity in calculated coverage amounts.

E. Residual Fluorine and Chlorine on 1/3 ML F- and Cl-Terminated Si(111) Surfaces after Ethylenediamine Treatment. Depending on the surface treatment, the Si−F and Si−Cl surfaces behave differently regarding the amounts of fluorine or chlorine left on the surface. For the Cl-terminated Si(111) surface (Figure 7 A and Table 1), liquid EDA at room temperature only removes 58% ± 3% of the Cl 2p peak, shifting the doublet from its starting 199 and 200.6 eV position on the fresh Si−Cl surface to 201.0 and 202.6 eV on the EDA treated surface. In comparison, all of the chlorine is reacted away after vapor phase EDA treatment with a surface temperature of 350 °C.

For the 1/3 ML F-terminated Si(111) surface (Figure 7B and Table 1), 10% ± 4% of the fluorine is left on the surface (∼0.03 ML of fluorine) after liquid EDA exposure. The remaining F 1s peak at 686.1 eV is slightly shifted from the XPS F 1s peak of the fresh 1/3 ML F-terminated Si(111) surface at 685.8 eV. In contrast to the Cl-terminated Si(111) surface, more F is left after the vapor EDA treatment, namely, 47% ± 9% of the original peak area is still on the surface, with the binding energy shifting to 687.5 eV after the exposure at 350 °C.

F. Comparison of Si−H Formation under Different Cl-Terminated Si(111) Surface Treatments. The vapor-phase EDA treatment allows for a more controlled reaction environment than liquid phase. Even though the vapor phase exposes a lower dosage of EDA to the surface, it still shows a strong and clear formation of Si−H bonds on the chlorinated surface. Figure 8D shows vibrational bands at 2060 and 623 cm^{-1} attributed to the stretch and deformation modes of SiH

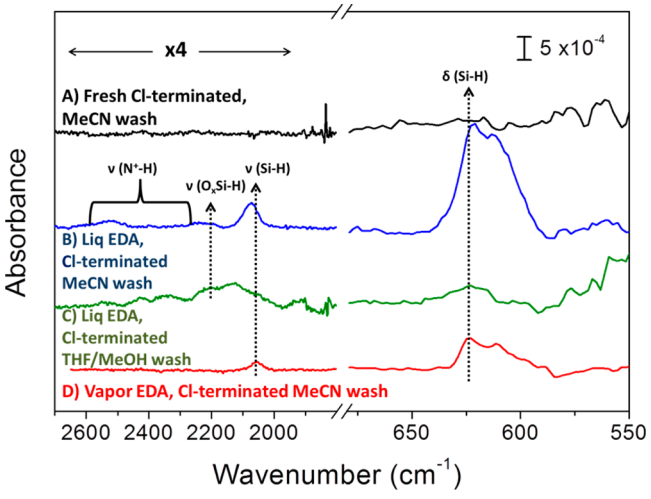

Figure 8. Infrared spectra of (A) fresh Cl-terminated Si(111) surface rinsed with chlorobenzene and acetonitrile, (B) liquid ethylenediamine reacted with a Cl-terminated Si(111) surface that was rinsed with chlorobenzene and acetonitrile prior to the amine reaction, (C) liquid ethylenediamine reacted with a Cl-terminated Si(111) surface that was rinsed with chlorobenzene, THF, and methanol prior to the amine reaction, and (D) vapor ethylenediamine reacted with a Cl-terminated Si(111) surface that was rinsed with chlorobenzene and acetonitrile prior to the amine reaction. The liquid EDA reactions were done at room temperature for 30 min under anhydrous conditions, while the vapor phase EDA was reacted at a surface temperature of 350 °C. All spectra are referenced to their respective oxide surface termination. Spectra in the 1700−2700 cm^{-1} region were enlarged 4× the original size for better clarity.

DOI: 10.1021/acs.chemmater.5b03156
Chem. Mater. XXXX, XXX, XXX−XXX

formed after vapor phase EDA exposure at 350 °C (none observed in Figure 8A), with an estimated coverage of 19% ± 1% SiH ML. There is also a band centered at 612 cm^{-1} assigned to the Si phonon, present due to a small difference in the temperature of the substrate between the sample before and after EDA treatment.

The results are more complex in the case of the liquid phase EDA treatment. For reference, the freshly prepared Cl-terminated Si(111) surface rinsed with chlorobenzene and acetonitrile is shown in Figure 8A and contains no trace of a hydrogen termination. When the chlorine surface is rinsed with chlorobenzene and acetonitrile prior to EDA exposure (Figure 8B), Si−H forms with an estimated 30% ± 6% SiH ML coverage once EDA is exposed to the surface. The Si−H moieties have a SiH stretch and deformation vibrational bands at 2070 and 620 cm^{-1}. This surface also suffers slight oxidation in the Si−H backbonds, evidenced by a weak band at 2245 cm^{-1} attributed to the stretch mode of Si−H with a backbonded oxide present and contains charged species (NH_2^+/ NH^+) characterized by vibrational features at 2525 cm^{-1} found in EDA dihydrochloride salts.[29]

When the Cl-terminated Si(111) surface is cleaned with chlorobenzene and THF prior to neat EDA exposure (Figure 8C), the concentration of Si−H bonds on oxide-free Si (2050 and 623 cm^{-1}) is reduced. Instead, two features at 2123 and 2224 cm^{-1} are present, assigned to Si−H moieties coordinated to one or two oxygen atoms, in good agreement to the 2113 and 2250 cm^{-1}, respective, literature values.[18] In addition, THF washing seems to cause more charging on the surface as evidenced by the vibrations at 2332 cm^{-1}, 2422 cm^{-1}, and 2538 cm^{-1} all attributed to N^+-H ---Cl^- hydrohalide salt vibrations. Even with the extra hydrohalide vibrations, this liquid EDA reaction still results in a 25% ± 2% SiH ML formation on the surface. Such hydrogen formation as a byproduct of an amine reaction on chlorinated Si surfaces has no precedent in the literature. It appears to be solely associated with Cl surface termination, as an increase in hydrogen amount is not observed for the 1/3 ML F surface termination. This can be confirmed by examining in detail the concentration of Si−H bonds prior to and after treatment of the 1/3 ML F- and 2/3 ML H-terminated Si(111) surface (see Figure S1). Therefore, the bond formation tentatively is attributed to a secondary reaction discussed during the Discussion section, involving EDA and remnant Si−Cl exchanging the Cl for a H on the surface.

4. DISCUSSION

A. EDA Attachment on H-, 1/3 ML F-, and Cl-Terminated Si(111) Surfaces. In this section, the EDA adsorption on the three distinct surfaces, H-, Cl-, and 1/3 ML F-terminated Si(111), is addressed and found to involve a range of interactions, such as weak physisorption, monodentate bonding through one amine end group, and bidentate (bridge) bonding involving both amine end groups.

i. H-Terminated Si(111) Surfaces. When EDA is exposed to H-terminated silicon surfaces (Figure 1B), the spectrum is characterized by a weak NH_2 scissor vibration at 1595 cm^{-1}, a weak ν(Si−N) stretch vibration at 825 cm^{-1}, and an intense absorption in the 1000−1200 cm^{-1} region attributed to ν(Si−O) stretch modes, possibly due to surface oxidation and obscuring any ν(C−N) vibrations. As sometimes observed for weakly adsorbed species and confirmed in the case of EDA, C−H infrared vibrations can appear weaker than expected as compared to other modes, even for a relatively thick layer. This is because the C−H vibrational intensity is strongly dependent on the local environment and orientation (see Figure S4). Altogether, these observations indicate that, under room temperature conditions, EDA does not significantly chemisorb on a H-terminated silicon surface. This conclusion is also supported by analyzing the N 1s XPS peak area in Figure 2A. The calculated N surface coverage contains almost a monolayer of charged EDA, while analysis of the Si^{1+} component shows that there is a negligible attachment (Si−N) on the surface. These observations confirm that EDA is physisorbed and not attached to the sample.

Since the extent of surface oxidation appears to correlate with the amount of physisorption, we speculate that the presence of oxide may foster EDA charging and physisorption during liquid phase processing, leading to the observed IR and XPS results. Further evidence of physisorption without reaction on the Si−H surface is seen in Figure 4 for lower EDA concentration (20 mM in toluene), where the IR absorption shows diamine adsorption, while no Si^{1+} is detectable in the Si 2p region, and more importantly, there is no contribution in the N 1s region. These observations suggest that EDA can physisorb and readily desorb from the surface in vacuum. Reaction with the lower EDA concentration also created an estimated 0.15 ± 0.01 nm SiO_2 layer, almost 10× lower than the neat EDA reaction (1.4 ± 0.6 nm). The 20 mM EDA solution also maintains 86% ± 5% of its starting hydrogen as opposed to only 19 ± 8% remaining for the neat EDA reaction (Table S1). This combination of lower surface oxidation and preservation of the hydrogen surface termination for the 20 mM EDA solution reaction is consistent with physisorption: with higher oxidation, there is more molecular physisorption, leading to the observation of molecular and charged species in XPS; for less extensive physisorption, as in the case of the 20 mM EDA solution reaction, the physisorbed molecules desorb in ultrahigh vacuum. DFT calculations in the next section account well for this behavior, showing that although EDA has a negligible physisorption energy to the Si−H surface, the kinetic barrier for the conversion of EDA physisorption to chemisorption still needs to be overcome. Because of the insignificant physisorption energy, if the kinetic barrier is not surpassed, the EDA molecule could desorb; all results would suggest that at room temperature, the kinetic energy barrier for the reaction is not reached.

ii. 1/3 ML F-Terminated Si(111) Surfaces. On the 1/3 ML F-terminated Si(111) surface (2/3 ML H-termination), a reaction clearly occurs. In fact, monodentate attachment (grafting of one end group of the molecule only) is suggested in Figure 1A with the observation of a clear ν(Si−N) stretch vibration at 825 cm^{-1} *and* evidence of a free NH_2 group: the presence of symmetric and antisymmetric NH_2 stretch modes at 3230 and 3350 cm^{-1} as well as the scissor NH_2 deformation mode at 1595 cm^{-1}.[58] There is also possible multilayering on the surface, as inferred from the higher than expected area of the N 1s XPS NH_2 component peak in Figure 2B: the intensity ratio of the N 1s components (NH_2/Si−N−C) is expected to be 1:1 if there is only monodentate attachment. The difference is therefore attributed to the presence of physisorbed EDA layers. Physisorbed layers screen electrons from the Si−N−C bond below (fortunately this bond is seen with IR spectroscopy). Consistent with this picture is the fact that the XPS of the EDA vapor phase experiment in Figure 6 (for which there is no physisorption) is dominated by the N 1s peak associated with the Si−N−C bond. The difference between the liquid and

DOI: 10.1021/acs.chemmater.5b03156
Chem. Mater. XXXX, XXX, XXX−XXX

gas phase experiments underscores the formation of multilayers in solution, in which charging and dative bonding occurs (Figure 2B). Such charging is not observed in the vapor phase experiment (Figure 6) as there is no evidence for multilayering. As on the H-terminated Si(111) surfaces, surface oxidation may foster the observed physisorption/multilayering. In both cases, surfaces are exposed to aqueous solutions during processing, unlike the anhydrous processing of the Cl-terminated Si(111) surface, allowing for trace amounts of water to physisorb on the surface. The trace amounts of water on the surface do not cause immediate oxidation to the fresh 1/3 ML F- or H-terminated Si(111) surface itself but could cause oxidation once the substrate is reacted with ethylenediamine.

Furthermore, due to the lower infrared peak intensities observed for the EDA vapor phase reaction as compared to the liquid phase and similarities in the ν(C−N) infrared band intensity for 1/3 ML F- and Cl-terminated EDA vapor phase reaction, it is inferred that little to no EDA physisorption has taken place in vapor phase. The lower pressure may also have removed the physisorbed water from the surface. More importantly, vapor phase EDA has an estimated ∼10× lower oxide thickness, supporting the theory of the correlation between oxidation and physisorption due to the presence of physisorbed water molecules. For XPS measurements, an additional source of surface oxidation could come from the brief sample air exposure during transport to the XPS chamber.

Although the vapor phase EDA experiment at 350 °C was only able to remove 47% ± 9% of the starting Si−F, the shift in the remaining Si−F to a higher binding energy (685.8 to 687.5 eV) is attributed to EDA chemisorption since a similar behavior is observed for fluorine species on a silicon nitride surface[4] and more covalently attached Si−F species.[60,61] Furthermore, the amount of hydrogen on the surface remains unchanged before and after the vapor phase EDA reaction and the sum of the coverage calculated for the Si−N−C species and remaining F 1s peak area match the roughly 1/3 monolayer coverage found from the Si^{1+} peak area. For liquid processing, the coverage of hydrogen is reduced (Table S1), likely due to oxidation. Also, Figure 7B and Table 1 show that fluorine is almost completely removed. Yet, the Si^{1+} component of the Si 2p peak remains constant, consistent with Si−F to Si−N conversion and suggesting that oxidation is mostly affecting the Si−H region.

Prior to air exposure, several observations indicate that vapor phase EDA adsorbs on the 1/3 ML F-terminated Si(111) surface in a monodentate configuration: the amount of hydrogen on the surface remains unchanged, with no EDA physisorption believed to occur, and there are marked differences in the 900−1600 cm^{-1} infrared region for vapor EDA on the 1/3 ML F- and Cl-terminated Si(111) surfaces, confirming that the bonding in each surface is very different.

Since no EDA physisorption is believed to take place for the vapor phase EDA reaction, the components of the XPS N 1s peak should now have a NH_2: Si−N−C area ratio of 1:1. However, as shown in the Results section, the experimental ratio of vapor phase EDA is 3:7. An explanation for this discrepancy in values could result from carbamic acid formation. It is known that amines react in air with CO_2 to create carbamate molecules or carbamates/carbamic acid.[62−65] The mechanism for carbamate/carbamic acid formation from ammonia air exposure, as found in Wang et al.,[63] is as follows:

$$CO_2(aq) + NH_3 \leftrightarrow NH_2COOH \quad (1)$$

$$NH_2CO_2^- + H^+ \leftrightarrow NH_2CO_2H \quad (2)$$

A similar process could potentially occur when the free ethylenediamine NH_2 end group is exposed to air, i.e., during transport to the XPS system. Therefore, a signature of carbamic acid could be observed in XPS as well.

The XPS C 1s region of the vapor EDA reacted with the 1/3 ML F- and Cl-terminated Si surfaces is shown in Figure S3. The 1/3 ML F-terminated Si(111) surface contains a small peak at 289 eV, attributed to C═O formation. As suggested in the Results section, the measured N 1s peak at 398 eV includes two contributions: (1) the Si−N−C bond from a monodentate attachment (Si-NH−CH_2−CH_2−NH_2) and (2) any reacted amine (e.g., carbamic acid) with C-NH-C bonding. The intensity ratio of the N 1s levels for the combined reacted amines and standard Si−N−C bonding of monodentate (∼398 eV) to the free monodentate NH_2 group (∼400 eV) is measured to be 2.3 (i.e., 7:3). This implies that 40% of the monodentate amine NH_2 moiety has been converted to carbamic acid upon air exposure. Since vapor phase experiments show no observable species in the XPS N 1s 401−402 eV region associated with amine charging, the presence of carbamate ions is ruled out. Consequently, we infer that the carbamic acid is formed instead.

We can also use the C 1s core level (shown in Figure S3) to confirm the carbamic acid hypothesis. For adsorbed carbamic acid, the expected ratio of the XPS N 1s signal to C 1s signal corresponding to the formation of Si-NH−CH_2−CH_2−NH−COOH species is 2/1. The experimentally derived ratio between the XPS N 1s 398 eV carbamic acid peak area to the observed C 1s C═O peak area is 1.9/1. Since the experimentally found ratio is close to the 2/1 expected ratio, it is concluded the monodentate-attached amines react to form carbamic acid (Si-NH−CH_2−CH_2−NH−COOH) on the surface when exposed to atmosphere.

iii. Cl-Terminated Si(111) Surfaces. Cl-terminated Si(111) surfaces are by far the most reactive. First, all the chlorine is completely removed during the vapor phase process as shown in Figure 7A and Table 1. Associated with this loss is the clear detection of Si−N vibrations after the vapor phase treatment (Figure 5). The spectral analysis of the liquid phase processes is more complex, as discussed below, because some Cl remains at the surface in the form of adsorbed salts and the Si−N vibration is part of a broader absorption band (Figure 1C). In fact, the reaction process is complex because chlorine products can play a role. Specifically, only 58% ± 3% of the Cl 2p peak appears to be removed for liquid phase processing (Figure 7) as opposed to the observed 100% removal for gas phase processing. This surprising observation is fully explained below by the redeposition of chlorine as a chloride salt.

Indeed, the position of the remaining Cl 2p peak for liquid phase is shifted toward a higher binding energy by 2 eV (now at 201 eV), indicative of a more covalent bond, such as found in hydrochloride salts. This suggestion is based on literature pointing to the formation of hydrohalide salts during amine−halide reactions.[66−69] This reaction involves a proton transfer from the hydrogen halide to the amine and is affected by the polarity of the nitrogen environment. Because of charge sharing, this salt-like state bears more characteristics of a covalently bonded network than the ionic nature of surface Si−Cl. In fact, the XPS Cl 2p peak in Figure 7 for the liquid phase EDA, (201 eV position) is similar to Cl 2p spectra measured in the case of aromatic amine polymers with HCl adducts

DOI: 10.1021/acs.chemmater.5b03156
Chem. Mater. XXXX, XXX, XXX−XXX

(polyaniline·HCl and *N,N′*-diphenyl-*p*-quinonediimine·HCl) having 2p 3/2 and 2p 1/2 peaks at 201.5 and 202 eV assigned to covalently bonded chlorine.[38] Further evidence of the XPS Cl 2p peak being a salt formation, comes from the peak found at 402.1 eV in the N 1s spectra for the liquid EDA, at the expected energy for a charged amine and in good agreement with the binding energy of NH_4Cl salt at 401 eV.[23] While the literature of liquid amine reactions on Cl-terminated surfaces[13,25,26] show complete chlorine removal, in this case the chlorine remained on the surface as a salt. It is worth noting that for vapor phase experiments (Figure 8D), there is no chlorine or charged amine signal observed in the N 1s spectra because these products are volatile. In fact, the vapor pressure of such salts would be comparable to NH_4Cl, which is 1.5 mTorr at 75 °C,[23] and therefore not present at the chamber pressure of $\sim 10^{-4}$ Torr. Furthermore, the substrate is kept at 350 °C during the reaction and at 80 °C during the IR measurements, precluding any possibility of salt physisorption. In contrast, during liquid phase processing, the infrared spectra in Figure 8B and C are characterized by N^+-H vibrations in the 2400−2700 cm^{-1} region[29,56,67] associated with amine hydrohalide salts.

Two new observations set apart the diamine reaction on Cl-terminated Si(111) surfaces: (1) evidence for bridge bonding and (2) formation of Si−H on the originally H-free surface, suggesting a secondary pathway after the original EDA grafting. The first point needs some elaboration, starting with the observation of new modes in the 1300−1500 cm^{-1} region, associated with CH_2 deformation modes, and only one ν(N−H) stretch vibration at 3300 cm^{-1}. The latter, coupled with lower absorption intensities in the 1000−1200 cm^{-1} region, imply the possibility of bridge bonding, with both ends of the molecule reacting with the surface. Note that the surface is less oxidized than the H- and 1/3 ML F-terminated Si(111) surfaces, in the case of both liquid and vapor phase processing. This observation is consistent with the estimation from the N 1s and Si^{1+} peak areas of an almost complete monolayer coverage of chemisorbed EDA for both vapor-phase and neat EDA processing. This almost full monolayer coverage means most of the chlorine sites (fully chlorinated surface reported to have 0.98 ML coverage)[46] have been reacted away and replaced by EDA. Finally, the presence of δ(N−H_2) in IR spectra (Figures 2A and 5) and an N 1s peak at ∼400 eV binding energy attributed to C-NH_2 indicates that there must be a mixture of bridging and monodentate (with a NH_2 end unreacted) attachment on the surface; however, the possibility of this binding energy containing minority amine oxide surface species, formed after air exposure, cannot be ruled out. The large discrepancy between the two XPS N 1s components (17:3), as well as the presence of the IR peak at 1112 cm^{-1} attributed to a secondary amine C−N bond and single vibration at 3340 cm^{-1} to a N−H stretch vibration, indicate that a majority of the surface is composed of Si-NH-C/NH-C bonds. Unlike the vapor phase 1/3 ML F-termination, in this case Figure S3 shows no evidence of a C═O bond formation upon air exposure; therefore, no carbamate/carbamic acid is formed before XPS analysis, and the N 1s 398.2 eV peak belongs only to the EDA bridging configuration, with a similar absence in C═O formation also observed in liquid phase (not shown).

The mechanisms for both novel observations are addressed theoretically in the next sections.

B. EDA Bridging on the Cl-Terminated Si(111) Surface. In order to gain insight into the differences in EDA reactivity with halogen- and hydrogen-terminated Si(111) surfaces, DFT calculations were performed to evaluate the minimum energy pathways (MEPs) linking reactant and product states. As discussed below, the estimated kinetic barriers are consistent with experimental observations: Si−H is less reactive than Si−Cl. The calculated kinetic energy contours shown in Figures 9

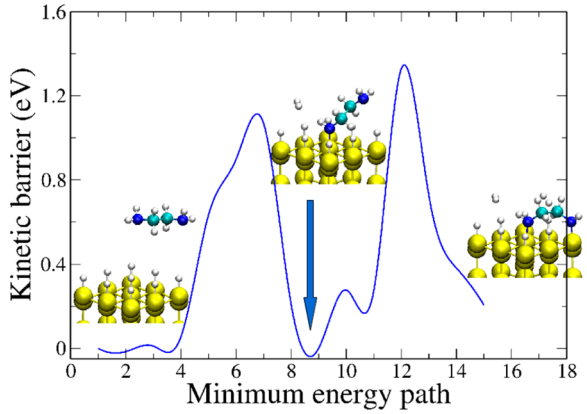

Figure 9. Kinetic barriers for the adsorption process of ethylenediamine (EDA) on the H-terminated Si(111) surface. The insets show the initial and final states of the single bond and bridge formation reactions, respectively. Yellow spheres represent Si atoms; white, H; turquoise, C; and blue spheres, N atoms.

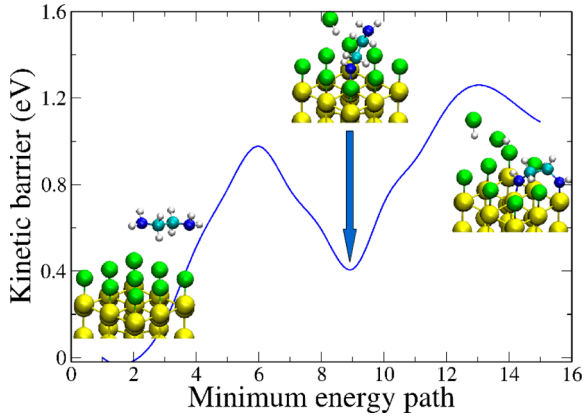

Figure 10. Kinetic barriers for the reaction of ethylenediamine (EDA) on the Cl-terminated Si(111) surface. The insets show the initial and final states for the single bond and bridge formation reactions, respectively. Yellow spheres represent Si atoms; green, Cl; white, H; turquoise, C; and blue spheres, N atoms.

and 10 indicate that the monodentate reaction products are the most thermodynamically favorable configuration for EDA adsorption for both H- and Cl-terminated Si(111) surfaces. Further reaction on the surface would produce the doubly reacted EDA bridging product (see Figures 9 and 10, and also Table S2). The DFT results also confirm the possibility (as discussed in the previous section for the Cl-Termination) of forming a mixture of monodentate and bridge structures on both the H- and Cl-terminated Si(111) surfaces because the estimated reaction enthalpies become more favorable when both structures are present on the surface (see Table S2).

To estimate the energetics for the formation of the monodentate and bridge configurations of the EDA on H-

DOI: 10.1021/acs.chemmater.5b03156
Chem. Mater. XXXX, XXX, XXX−XXX

and Cl-terminated Si(111) surfaces, we obtained the energetics for EDA reaction, starting from the initial desorbed configuration to the final fully reacted structures. These reaction pathways are illustrated in Figures 9 and 10, where we show the calculated kinetic barriers as the highest energy configurations along the minimum energy path. These kinetic barriers present the upper-bounds for the activation energies and highlight important differences between the two substrates.

The pictures in the insets of Figures 9 and 10 show the respective initial, single bond (monodentate), and bridge configurations for reaction of EDA in the gas phase. Several considerations are in order: first, as the molecule impinges on both H- and Cl-terminated Si(111) surfaces, it undergoes physisorption without a kinetic barrier or thermodynamic (~0.05 eV) barrier. This ease of physisorption indicates that unless sufficient energy is available to overcome the kinetic barrier for monodentate formation (~1.2 eV and ~1.0 eV for H-terminated and Cl-terminated Si(111) surfaces, respectively), the EDA molecule would easily desorb. Second, although the EDA single bond formation is slightly exothermic (−0.01 eV) for a H-terminated Si(111) surface and endothermic for the Cl-terminated Si(111) surface (0.41 eV), the opposite is true for bridge formation on the two surfaces. For the second step of the reaction (bridge formation), the kinetic barrier of the Cl-terminated Si(111) is lower than that for the H-terminated surface (0.85 eV vs 1.32 eV). Therefore, the single-bond formation is the rate-limiting reaction step, with the EDA bridge formation occurring preferentially on the Cl-terminated surface, even if thermodynamically not preferred.

From an experimental point of view, EDA bridging on silicon has only previously been observed for EDA reactions on bare Si (100) 2 × 1 surfaces.[59] Interestingly, the strain associated with the bridge configuration on the Cl-terminated Si(111) surface enhances the infrared absorption of vibrations that could previously not be detected, such as the $\delta_{twist}(C-H_2)$, $\delta_{wag}(N-H)$, and $\delta(C-H_2)$ deformation modes, which are now visible in the IR spectra. In comparison to the 1/3 ML F-termination, the CH_2 deformation bands of the Cl-terminated Si(111) surfaces for both liquid and vapor-phase processing are more intense. This change in intensity of the CH_2 deformation modes has also been reported in the literature, in the infrared of ring structures containing nitrogen groups, such as pyrrolidine,[70] a five-member ring with one nitrogen, and piperazine,[37,70,71] a six-member ring with two nitrogen atoms, analogous of a bridge reaction between two ethylenediamine molecules. The formation of a bridge configuration on the Cl-terminated Si(111) surface is inferred from similar infrared vibrations in the 1300−1500 cm^{-1} region for the ring structures and the current data (Figure 1C and Figure 5), and from the dominant N 1s XPS peak at 398.5 eV (86% of the N 1s peak) in Figure 2A and Figure 5, attributed to Si−N−C binding. Furthermore, the calculated intensities for the IR absorption bands of both the monodentate and bridging structures (see Table S3) are also consistent with the formation of bridging EDA. In summary, the specific fingerprints of the bridging configuration, such as the different IR activities of CH_2 modes and shift of the C−N stretch mode, support the conclusion that a portion of the adsorbed EDA on Cl-terminated Si(111) surfaces is in a bridge bonding configuration.

C. Hydrogen Formation on the Cl-Terminated Si(111) Surface after EDA Exposure. None of the reported experiments with vapor phase reactions of amines on the Si(100)-Cl surface[22−24] or wet-chemical amine reactions on Si(111)[25−27] have noticed the formation of Si−H as a surface product. The only literature evidence found for Si−H formation comes from the decomposition of ammonia molecules on bare Si(100) 2 × 1 or Si(111) 7 × 7 surfaces,[11,14,18−20,69] i.e., the amine breaks apart forming Si−H and Si-NH_2 bonds.

To account for the observed Si−H formation on Cl-terminated Si(111) surfaces upon EDA treatment, DFT was used to calculate the reaction energies for two of the most likely pathways. The first pathway, with a reaction enthalpy of +3.07 eV, uses the HCl byproduct of the monodentate EDA attachment,

$$H_2N\text{-}(CH_2)_2\text{-}NH_2 + \text{Si-Cl} \rightarrow \text{Si-NH-}(CH_2)_2\text{-}NH_2 + HCl \quad (3)$$

and the HCl reacts with a neighboring Si−Cl bond, creating $Cl_2(g)$ and Si−H on the surface.

$$HCl + \text{Si-Cl} \rightarrow \text{Si-H} + Cl_2 \quad (4)$$

The second pathway, being endothermic by +2.30 eV, involves a proton−chlorine exchange between the chlorinated surface and the EDA molecule, with the resulting NH_2-$(CH_2)_2$-NHCl molecule leaving the surface.

$$H_2N\text{-}(CH_2)_2\text{-}NH_2 + \text{Si-Cl} \rightarrow \text{Si-H} + NH_2\text{-}(CH_2)_2\text{-}NHCl \quad (5)$$

Both pathways are therefore thermodynamically unfavorable (see Table S2), having significant endothermic energies. While both schemes are endothermic, the second reaction is less unfavorable and could become enhanced by the initial attachment of EDA to the surface. Table S2 shows that the reaction enthalpy is lowered by the presence of functionalized neighboring sites, assisted by concerted chemical reactions. Therefore, either or both processes could facilitate the formation of Si-H on the surface possible at room temperature in solution and at 350 °C in vapor phase. To confirm such possibilities, we calculated the IR spectra of a surface resulting from this proton−chlorine exchange reaction. Our calculated wavenumbers for the Si−H stretch and deformation modes are at 2080 and 609 cm^{-1}, respectively, in good agreement with the experimental data discussed below.

The Si−H stretching and bending vibrations are observed at 2060 and 622 cm^{-1}, respectively, after vapor EDA exposure to a Cl-terminated Si(111) surface (Figure 5). In comparison, a fresh H-termination contains a sharp stretch vibration at 2083 cm^{-1} with its deformation mode found at 626 cm^{-1}, both of similar frequencies to the observed vibrations of the vapor phase reaction. These frequencies are consistent with the Si−H modes of ammonia dissociated on a Si(111) 7 × 7 bare surface reported by Colaianni et al.:[18] stretching mode at 2060 cm^{-1} and bending mode at 620 cm^{-1}, and are consistent with *isolated* Si−H bonds on Si(111) surfaces. Similar stretching and bending modes have also been observed for ammonia dissociation on bare Si (100) 2 × 1.[12,15] For the vapor phase EDA experiment in Figure 5, a 19% ± 1% ML Si−H coverage is estimated using the Si−H stretching mode of the H-terminated Si(111) surface. Note that liquid phase EDA experiments on Cl-terminated Si(111) surfaces show slightly higher coverages of Si−H, the amount depending on the solvent used for rinsing the fresh Cl-terminated Si(111) surface prior to diamine exposure. For instance, Cl-terminated Si(111) surfaces rinsed with THF show 25% ± 2% SiH formation, with Si−H

DOI: 10.1021/acs.chemmater.5b03156
Chem. Mater. XXXX, XXX, XXX−XXX

stretching and bending vibrations located at 2050 and 623 cm^{-1}, respectively. In comparison, solvents leading to less hydrohalide salt formation such as acetonitrile lead to 30% ± 6% SiH formation with SiH stretching and bending vibrational bands at 2070 and 620 cm^{-1}. Between the two types of rinsing, the acetonitrile-rinsed Cl-terminated Si(111) surfaces (Figure 8B) contained only one hydrohalide salt vibration, at 2525 cm^{-1}, and less oxidation (less intense $O_3 \equiv Si-H$ vibration at 2245 cm^{-1}) after EDA exposure.

D. Possibility of Nitridation with Vapor and Liquid Phase EDA Processing. Since it is difficult to distinguish silicon nitride (or oxynitride) from silicon oxide based on XPS data, we address the potentiality for nitridation of the silicon surface during EDA functionalization using IR spectroscopic data instead. The first observation in Figures 4, 5, 6, and 8 is that all of the Si−H stretch modes are located either at ∼2100 cm^{-1} or in the 2250−2260 cm^{-1} region, the latter being typical of Si−H with oxygen in its backbonds (i.e., oxidized silicon). If nitridation occurred on surfaces with some H-termination, infrared absorption bands would be expected at 2169 or 2212 cm^{-1} corresponding to backbonded SiN_2−Si-H and N_3−Si-H, respectively, would be observed.[21] Also, depending on the degree of nitridation, broad Si−N−Si infrared phonon bands[4,21] would be observed at ∼800−840 cm^{-1} and ∼1050−1140 cm^{-1}, along with an associated bending, δ(N−H), mode at 1180 cm^{-1} arising from the insertion of N atoms into the Si-SiH backbond. If defect sites of H-terminated Si(111) surfaces were to react, forming a silazane H-Si-NH-Si bridging structure for instance, a band at 775 cm^{-1} would be observed, corresponding to the N−H bending vibration.[21] Instead, irrespective of the EDA exposure method (vapor or liquid phase), all surface terminations develop a vibration in the 2250−2260 cm^{-1} region, i.e., higher than expected for purely N insertion into SiH backbonds of H-terminated Si(111) surfaces. Even the purely Cl-terminated Si(111) surface develops a partial H-termination, as discussed in section D, with two features at 2123 and 2224 cm^{-1} (Figures 8C and S1C). If these bands were associated with N insertion into the silicon backbonds, i.e., SiN_2−Si-H and N_3−Si-H, then there should be well-defined phonon modes in the ∼800−840 cm^{-1} and ∼1050−1140 cm^{-1} regions associated with silicon nitride. According to Figure 1C, the Cl-termination has weak vibrations at 800 and 1130 cm^{-1}, likely belonging to the C−N stretch mode, with no evidence of a peak around 1180 cm^{-1}. On the basis of the intensity of the modes found at 2123 and 2224 cm^{-1}, a significantly stronger phonon region is expected. In addition, if the ∼800−840 cm^{-1} and ∼1050−1140 cm^{-1} bands originated from surface nitridation, the vapor phase EDA spectrum in Figure 5 would show a similar behavior. Instead, the vapor phase EDA spectrum has δ(NH) bands at 980 and 895 cm^{-1} and a band at 1112 cm^{-1} characteristic of a secondary ν(C−N) amines, with no contribution in the 2100−2400 cm^{-1} region. Theoretically, although EDA nitridation is possible, it is shown to be thermodynamically unfavorable with reaction energies in the range of 2.3−2.7 eV. DFT calculations show that for Si−N−Si backbonds to form, the monodentate-attached EDA on the Cl-terminated Si(111) surface must break the C−N bond and form a C−N−C 3-membered ring on the surface (see Figure S2). Despite its similar thermodynamic energy to that of hydrogen formation on the Cl-terminated Si(111) surface (2.3 eV), nitridation likely has a higher kinetic energy barrier than hydrogen formation since dissociation of the C−N bond and formation of a strained C−N−C 3-membered ring are involved. The nitridation kinetic barrier is possibly the driving force in preventing nitridation on the surface. Altogether, the lack of broad and strong of silicon nitride bands in the phonon region (∼800−840 cm^{-1} and ∼1050−1140 cm^{-1}) and in the 2100−2240 cm^{-1} region for the H- and 1/3 ML F-terminated Si(111) surfaces is not consistent with nitridation. Furthermore, the observed N 1s XPS binding energies (∼398 and 400 eV) are also not supportive of nitridation; the silicon nitride N 1s binding energy is usually found around 396.7−397.5 eV range, although it is known to be shifted to higher binding energies in the presence of electron withdrawing groups, such as F, Cl, and O. If the nitrogen moiety observed at ∼398.1 eV contained nitride species, N_x−Si-H vibrational modes would be expected to be present in the infrared spectra since hydrogen was either present before or after the EDA functionalization on the surface. The lack of vibrations in the N_x−Si-H mode region for the EDA liquid phase H- and 1/3 ML F-terminated Si(111) surfaces and EDA vapor phase 1/3 ML F- and Cl-terminated Si(111) surfaces rules out nitridation. Therefore, the species found in the 102.5−103.3 eV spectra of the XPS Si 2p and the vibrations observed in the 2100−2400 cm^{-1} region of the Cl- terminated liquid EDA reaction are solely be attributed to oxide formation.

■ CONCLUSIONS

In summary, we have shown that the initial termination of oxide-free silicon surfaces plays a key role in the EDA chemisorption and the final configuration of adsorbed EDA at the surface. Specifically, EDA shows negligible chemisorption on the H-terminated Si(111) surface for all EDA concentrations (neat to dilute). In contrast, a monodentate attachment is observed for 1/3 ML F-terminated Si(111) surfaces upon both liquid and vapor-phase EDA processing. EDA is most reactive on Cl-terminated Si(111) surfaces on which it can bond in a bridge configuration, as evidenced by characteristic IR absorption bands and N 1s binding energies. Such a configuration has not previously been observed for EDA reactions on modified silicon surfaces, but only seen under UHV conditions for bare silicon. An unexpected hydrogenation of the initially fully Cl-terminated Si(111) surface is also observed, and tentatively attributed to a proton exchange mechanism upon reaction of EDA with the Si−Cl bond. An alternative mechanism involving the participation of the HCl product is also considered although thermodynamically less favorable. Diamine modification of oxide-free surfaces is therefore possible and, upon process optimization, could open up new manufacturing possibilities for future silicon-based devices.

■ ASSOCIATED CONTENT

Supporting Information

The Supporting Information is available free of charge on the ACS Publications website at DOI: 10.1021/acs.chemmater.5b03156.

Infrared spectra and summary table of SiH from neat EDA, DFT reaction barriers of surfaces, DFT and experimental EDA infrared vibrations, DFT configurations of silicon nitride formation, carbamic acid formation for vapor-phase EDA, infrared EDA multilayer formation on H-termination, and XPS thickness and coverage calculation methods (PDF)

DOI: 10.1021/acs.chemmater.5b03156
Chem. Mater. XXXX, XXX, XXX−XXX

AUTHOR INFORMATION

Corresponding Author

*E-mail: chabal@utdallas.edu.

Notes

The authors declare no competing financial interest.

ACKNOWLEDGMENTS

This work was supported by the National Science Foundation (Grant CHE-1300180), and calculations were done in TACC.

REFERENCES

(1) Caillard, L.; Sattayaporn, S.; Lamic-Humblot, A.-F.; Casale, S.; Campbell, P.; Chabal, Y. J.; Pluchery, O. Controlling the reproducibility of Coulomb blockade phenomena for gold nanoparticles on an organic monolayer/silicon system. *Nanotechnology* **2015**, *26*, 065301.

(2) Yang, Z. K.; Song, L. X.; Teng, Y.; Xia, J. Ethylenediamine-modulated synthesis of highly monodisperse copper sulfide microflowers with excellent photocatalytic performance. *J. Mater. Chem. A* **2014**, *2*, 20004−20009.

(3) Wu, M.; Rhee, J.; Emge, T. J.; Yao, H.; Cheng, J.-H.; Thiagarajan, S.; Croft, M.; Yang, R.; Li, J. A low band gap iron sulfide hybrid semiconductor with unique 2D [Fe16S20]8- layer and reduced thermal conductivity. *Chem. Commun.* **2010**, *46*, 1649−1651.

(4) Liu, L.-H.; Debenedetti, W. J. I.; Peixoto, T.; Gokalp, S.; Shafiq, N.; Veyan, J.-F.; Michalak, D. J.; Hourani, R.; Chabal, Y. J. Morphology and chemical termination of HF-etched Si3N4 surfaces. *Appl. Phys. Lett.* **2014**, *105*, 261603.

(5) Seitz, O.; Fernandes, P. G.; Tian, R.; Karnik, N.; Wen, H.-C.; Stiegler, H.; Chapman, R. A.; Vogel, E. M.; Chabal, Y. J. Control and stability of self-assembled monolayers under biosensing conditions. *J. Mater. Chem.* **2011**, *21*, 4384−4392.

(6) Aureau, D.; Varin, Y.; Roodenko, K.; Seitz, O.; Pluchery, O.; Chabal, Y. J. Controlled Deposition of Gold Nanoparticles on Well-Defined Organic Monolayer Grafted on Silicon Surfaces. *J. Phys. Chem. C* **2010**, *114*, 14180−14186.

(7) Schmidt, N. W.; Jin, F.; Lande, R.; Curk, T.; Xian, W.; Lee, C.; Frasca, L.; Frenkel, D.; Dobnikar, J.; Gilliet, M.; Wong, G. C. L. Liquid-crystalline ordering of antimicrobial peptide-DNA complexes controls TLR9 activation. *Nat. Mater.* **2015**, *14*, 696−700.

(8) Lapin, N. A.; Chabal, Y. J. Infrared Characterization of Biotinylated Silicon Oxide Surfaces, Surface Stability, and Specific Attachment of Streptavidin. *J. Phys. Chem. B* **2009**, *113*, 8776−8783.

(9) Yaacobi-Gross, N.; Soreni-Harari, M.; Zimin, M.; Kababya, S.; Schmidt, A.; Tessler, N. Molecular control of quantum-dot internal electric field and its application to CdSe-based solar cells. *Nat. Mater.* **2011**, *10*, 974−979.

(10) Tang, H.; Yan, M.; Zhang, H.; Xia, M.; Yang, D. Preparation and characterization of water-soluble CdS nanocrystals by surface modification of ethylene diamine. *Mater. Lett.* **2005**, *59*, 1024−1027.

(11) Mathieu, C.; Bai, X.; Bournel, F.; Gallet, J. J.; Carniato, S.; Rochet, F.; Sirotti, F.; Silly, M. G.; Chauvet, C.; Krizmancic, D.; Hennies, F. Nitrogen 1s NEXAFS and XPS spectroscopy of NH_3-saturated Si(100)- 2 × 1: Theoretical predictions and experimental observations at 300 K. *Phys. Rev. B: Condens. Matter Mater. Phys.* **2009**, *79*, 205317.

(12) Queeney, K.; Chabal, Y.; Raghavachari, K. Role of Interdimer Interactions in NH3 Dissociation on Si(100)-(2 × 1). *Phys. Rev. Lett.* **2001**, *86*, 1046−1049.

(13) Zhu, X. Y.; Mulder, J. A.; Bergerson, W. F. Chemical Vapor Deposition of Organic Monolayers on Si(100) via Si−N Linkages. *Langmuir* **1999**, *15*, 8147−8154.

(14) Cao, X.; Hamers, R. Silicon Surfaces as Electron Acceptors: Dative Bonding of Amines with Si(100) and Si(111) Surfaces. *J. Am. Chem. Soc.* **2001**, *123*, 10988−10996.

(15) Rodríguez-Reyes, J.; Teplyakov, A. Cooperative nitrogen insertion processes: Thermal transformation of N H 3 on a Si (100) surface. *Phys. Rev. B: Condens. Matter Mater. Phys.* **2007**, *76*, 075348.

(16) Naitabdi, A.; Bournel, F.; Gallet, J.-J.; Markovits, A.; Rochet, F.; Borensztein, Y.; Silly, M. G.; Sirotti, F. Triethylamine on Si(001)-(2 × 1) at 300 K: Molecular Adsorption and Site Configurations Leading to Dissociation. *J. Phys. Chem. C* **2012**, *116*, 16473−16486.

(17) Finstad, C. C.; Muscat, A. J. Ammonia Photodissociation Promoted by Si(100). *J. Phys. Chem. A* **2014**, *118*, 3880−3890.

(18) Colaianni, M. L.; Chen, P. J.; Yates, J. T. The stepwise dissociation of NH_3 on the Si(11)-(7 × 7) surface: Low-temperature dissociative adsorption and thermal effects. *J. Chem. Phys.* **1992**, *96*, 7826−7837.

(19) Björkqvist, M.; Göthelid, M.; Grehk, T. M.; Karlsson, U. O. NH_3 on Si(111)7 × 7: Dissociation and surface reactions. *Phys. Rev. B: Condens. Matter Mater. Phys.* **1998**, *57*, 2327−2333.

(20) Cao, X.; Hamers, R. Molecular and dissociative bonding of amines with Si(111)-(7 × 7) surfaces. *Surf. Sci.* **2003**, *523*, 241−251.

(21) Dai, M.; Wang, Y.; Kwon, J.; Halls, M. D.; Chabal, Y. J. Nitrogen interaction with hydrogen-terminated silicon surfaces at the atomic scale. *Nat. Mater.* **2009**, *8*, 825−830.

(22) Lee, H. S.; Choi, C. H. Adsorption Mechanisms of NH3 on Chlorinated Si(100)-2 × 1 Surface. *Bull. Korean Chem. Soc.* **2012**, *33*, 775.

(23) Finstad, C. C.; Thorsness, A. G.; Muscat, A. J. The mechanism of amine formation on Si(100) activated with chlorine atoms. *Surf. Sci.* **2006**, *600*, 3363−3374.

(24) Bergerson, W. F.; Mulder, J. A.; Hsung, R. P.; Zhu, X. Y. Assembly of Organic Molecules on Silicon Surfaces via the Si−N Linkage. *J. Am. Chem. Soc.* **1999**, *121*, 454−455.

(25) Cui, Y. X.; Tian, F. Y.; Gao, F.; Teplyakov, A. V. Building Organic Monolayers Based on Fluorinated Amines on the Si(111) Surface. *J. Phys. Chem. C* **2014**, *118*, 26721−26728.

(26) Gao, F.; Teplyakov, A. V. Reaction of Hydrazine with a Chlorine-Terminated Si(111) Surface. *J. Phys. Chem. C* **2014**, *118*, 27998−28006.

(27) Tian, F.; Taber, D. F.; Teplyakov, A. V. −NH− Termination of the Si(111) Surface by Wet Chemistry. *J. Am. Chem. Soc.* **2011**, *133*, 20769−20777.

(28) Allen, A. D.; Senoff, C. V. Infrared spectra of tris-ethylenediamine complexes of ruthenium (II). *Can. J. Chem.* **1965**, *43*, 888−895.

(29) Baldwin, M. E. 848. The infrared spectra of cobalt(III) ethylenediamine complexes. Part I. Vibrations of the ethylenediamine chelate ring. *J. Chem. Soc.* **1960**, 4369−4376.

(30) Inokuma, Y.; Yoshioka, S.; Ariyoshi, J.; Arai, T.; Hitora, Y.; Takada, K.; Matsunaga, S.; Rissanen, K.; Fujita, M. X-ray analysis on the nanogram to microgram scale using porous complexes. *Nature* **2013**, *495*, 461−466.

(31) Choi, S.; Watanabe, T.; Bae, T.-H.; Sholl, D. S.; Jones, C. W. Modification of the Mg/DOBDC MOF with Amines to Enhance CO2 Adsorption from Ultradilute Gases. *J. Phys. Chem. Lett.* **2012**, *3*, 1136−1141.

(32) Chen, C.; Kim, J.; Park, D.-W.; Ahn, W.-S. Ethylenediamine grafting on a zeolite-like metal organic framework (ZMOF) for CO2 capture. *Mater. Lett.* **2013**, *106*, 344−347.

(33) Lee, W. R.; Hwang, S. Y.; Ryu, D. W.; Lim, K. S.; Han, S. S.; Moon, D.; Choi, J.; Hong, C. S. Diamine-functionalized metal-organic framework: exceptionally high CO2 capacities from ambient air and flue gas, ultrafast CO2 uptake rate, and adsorption mechanism. *Energy Environ. Sci.* **2014**, *7*, 744−751.

(34) Herlem, G.; Goux, C.; Fahys, B.; Dominati, F.; Gonçalves, A. M.; Mathieu, C.; Sutter, E.; Trokourey, A.; Penneau, J. F. Surface modification of platinum and gold electrodes by anodic oxidation of pure ethylenediamine. *J. Electroanal. Chem.* **1997**, *435*, 259−265.

(35) Herlem, G.; Reybier, K.; Trokourey, A.; Fahys, B. Electrochemical Oxidation of Ethylenediamine: New Way to Make Polyethyleneimine-Like Coatings on Metallic or Semiconducting Materials. *J. Electrochem. Soc.* **2000**, *147*, 597−601.

DOI: 10.1021/acs.chemmater.5b03156
Chem. Mater. XXXX, XXX, XXX−XXX

(36) Herlem, M.; Fahys, B.; Herlem, G.; Lakard, B.; Reybier, K.; Trokourey, A.; Diaco, T.; Zairi, S.; Jaffrezic-Renault, N. Surface modification of p-Si by a polyethylenimine coating: influence of the surface pre-treatment. Application to a potentiometric transducer as pH sensor. *Electrochim. Acta* **2002**, *47*, 2597−2602.
(37) Spell, H. L. Determination of piperazine rings in ethyleneamines, poly(ethyleneamine), and polyethylenimine by infrared spectrometry. *Anal. Chem.* **1969**, *41*, 902−905.
(38) Hagiwara, T.; Demura, T.; Iwata, K. Synthesis and properties of electrically conducting polymers from aromatic amines. *Synth. Met.* **1987**, *18*, 317−322.
(39) Burrows, V. A.; Chabal, Y. J.; Higashi, G. S.; Raghavachari, K.; Christman, S. B. Infrared spectroscopy of Si(111) surfaces after HF treatment: Hydrogen termination and surface morphology. *Appl. Phys. Lett.* **1988**, *53*, 998−1000.
(40) Chabal, Y. J.; Higashi, G. S.; Raghavachari, K.; Burrows, V. A. Infrared spectroscopy of Si(111) and Si(100) surfaces after HF treatment: Hydrogen termination and surface morphology. *J. Vac. Sci. Technol., A* **1989**, *7*, 2104−2109.
(41) Higashi, G. S.; Chabal, Y. J.; Trucks, G. W.; Raghavachari, K. Ideal hydrogen termination of the Si (111) surface. *Appl. Phys. Lett.* **1990**, *56*, 656−658.
(42) Michalak, D. J.; Amy, S. R.; Aureau, D.; Dai, M.; Esteve, A.; Chabal, Y. J. Nanopatterning Si(111) surfaces as a selective surface-chemistry route. *Nat. Mater.* **2010**, *9*, 266−271.
(43) Bansal, A.; Li, X.; Lauermann, I.; Lewis, N. S.; Yi, S. I.; Weinberg, W. H. Alkylation of Si Surfaces Using a Two-Step Halogenation/Grignard Route. *J. Am. Chem. Soc.* **1996**, *118*, 7225−7226.
(44) Webb, L. J.; Nemanick, E. J.; Biteen, J. S.; Knapp, D. W.; Michalak, D. J.; Traub, M. C.; Chan, A. S. Y.; Brunschwig, B. S.; Lewis, N. S. High-Resolution X-ray Photoelectron Spectroscopic Studies of Alkylated Silicon(111) Surfaces. *J. Phys. Chem. B* **2005**, *109*, 3930−3937.
(45) Jakob, P.; Chabal, Y. J. Chemical etching of vicinal Si(111): Dependence of the surface structure and the hydrogen termination on the pH of the etching solutions. *J. Chem. Phys.* **1991**, *95*, 2897−2909.
(46) Rivillon, S.; Chabal, Y. J.; Webb, L. J.; Michalak, D. J.; Lewis, N. S.; Halls, M. D.; Raghavachari, K. Chlorination of hydrogen-terminated silicon (111) surfaces. *J. Vac. Sci. Technol., A* **2005**, *23*, 1100−1106.
(47) Himpsel, F. J. M.; Taleb-Ibrahimi, A.; Yarmoff, J. A.; Hollinger, G. Microscopic structure of the SiO_2/Si interface. *Phys. Rev. B: Condens. Matter Mater. Phys.* **1988**, *38*, 6084−6096.
(48) Blöchl, P. E. Projector augmented-wave method. *Phys. Rev. B: Condens. Matter Mater. Phys.* **1994**, *50*, 17953−17979.
(49) Kresse, G.; Furthmüller, J. Efficiency of Ab-Initio Total Energy Calculations for Metals and Semiconductors Using a Plane-Wave Basis Set. *Comput. Mater. Sci.* **1996**, *6*, 15−50.
(50) Kresse, G.; Hafner, J. Ab initio molecular dynamics for open-shell transition metals. *Phys. Rev. B: Condens. Matter Mater. Phys.* **1993**, *48*, 13115−13118.
(51) Perdew, J. P.; Burke, K.; Ernzerhof, M. Generalized Gradient Approximation Made Simple. *Phys. Rev. Lett.* **1996**, *77*, 3865−3868.
(52) Monkhorst, H. J.; Pack, J. D. Special Points for Brillouin-Zone Integrations. *Phys. Rev. B* **1976**, *13*, 5188−5192.
(53) Henkelman, G.; Jónsson, H. Improved tangent estimate in the nudged elastic band method for finding minimum energy paths and saddle points. *J. Chem. Phys.* **2000**, *113*, 9978−9985.
(54) Henkelman, G.; Uberuaga, B. P.; Jónsson, H. A climbing image nudged elastic band method for finding saddle points and minimum energy paths. *J. Chem. Phys.* **2000**, *113*, 9901−9904.
(55) Jónsson, H.; Mills, G.; Jacobsen, K. W. *Classical and Quantum Dynamics in Condensed Phase Simulations*; World Scientific Press: Singapore, 1998.
(56) Socrates, G. *Infrared and Raman Characteristic Group Frequencies: Tables and Charts*. 3rd ed.; John Wiley & Sons, LTD: Chichester: England, 2001.
(57) Reusch, W. Amines. https://www2.chemistry.msu.edu/faculty/reusch/virttxtjml/spectrpy/InfraRed/irspec1.htm (accessed Oct 1 2014).
(58) Giorgini, M. G.; Pelletti, M. R.; Paliani, G.; Cataliotti, S. Vibrational Specta and Assigments of Ethylene-Diamine and its Deuterated Derivatives. *J. Raman Spectrosc.* **1983**, *14*, 16−21.
(59) Mathieu, C.; Bai, X.; Gallet, J. J.; Bournel, F.; Carniato, S.; Rochet, F.; Magnano, E.; Bondino, F.; Funke, R.; Köhler, U.; Kubsky, S. Molecular Staples on Si(001)-2 × 1: Dual-Head Primary Amines. *J. Phys. Chem. C* **2009**, *113*, 11336−11345.
(60) Lippold, M.; Böhme, U.; Gondek, C.; Kronstein, M.; Patzig-Klein, S.; Weser, M.; Kroke, E. Etching Silicon with HF−HNO3−H2SO4/H2O Mixtures − Unprecedented Formation of Trifluorosilane, Hexafluorodisiloxane, and Si−F Surface Groups. *Eur. J. Inorg. Chem.* **2012**, *2012*, 5714−5721.
(61) Takahagi, T.; Ishitani, A.; Kuroda, H.; Nagasawa, Y. Fluorine-containing species on the hydrofluoric acid etched silicon single-crystal surface. *J. Appl. Phys.* **1991**, *69*, 803−807.
(62) Schaefer, W. H. Reaction of primary and secondary amines to form carbamic acid glucuronides. *Curr. Drug Metab.* **2006**, *7*, 873−881.
(63) Wang, X.; Conway, W.; Fernandes, D.; Lawrance, G.; Burns, R.; Puxty, G.; Maeder, M. Kinetics of the Reversible Reaction of CO2(aq) with Ammonia in Aqueous Solution. *J. Phys. Chem. A* **2011**, *115*, 6405−6412.
(64) Serna-Guerrero, R.; Da'na, E.; Sayari, A. New Insights into the Interactions of CO2 with Amine-Functionalized Silica. *Ind. Eng. Chem. Res.* **2008**, *47*, 9406−9412.
(65) Sayari, A.; Belmabkhout, Y. Stabilization of Amine-Containing CO2 Adsorbents: Dramatic Effect of Water Vapor. *J. Am. Chem. Soc.* **2010**, *132*, 6312−6314.
(66) Brissette, C.; Sandorfy, C. Hydrogen bonding in the amine hydrohalides: II. The infrared spectrum from 4000 to 2200 cm^{-1}. *Can. J. Chem.* **1960**, *38*, 34−44.
(67) Chenon, B.; Sandorfy, C. Hydrogen bonding in the amine hydrohalides: I. General aspects. *Can. J. Chem.* **1958**, *36*, 1181−1206.
(68) Lussier, L. S.; Sandorfy, C.; Le Thanh, H.; Vocelle, D. Effect of acids on the infrared spectra of the Schiff base of trans-retinal. *J. Phys. Chem.* **1987**, *91*, 2282−2287.
(69) Mielke, Z.; Barnes, A. J. Infrared matrix isolation studies of complexes between N,N-dimethylacetamide and hydrogen halides. Part 1.-Hydrogen chloride and hydrogen bromide complexes. *J. Chem. Soc., Faraday Trans. 2* **1986**, *82*, 437−446.
(70) El-Gogary, T. M.; Soliman, M. S. Ab-Initio molecular geometry andd normal coordinate analysis of pyrrolidine molecule. *Spectrochim. Acta, Part A* **2001**, *57*, 2647−2657.
(71) Gunasekaran, S.; Anita, B. Spectral investigation and normal coordinate analysis of piperazine. *Indian J. Pure Appl. Phys.* **2008**, *46*, 833−838.

DOI: 10.1021/acs.chemmater.5b03156
Chem. Mater. XXXX, XXX, XXX−XXX